Al-Khwarizmi Engineering Journal
ISSN (printed): 1818 – 1171, ISSN (online): 2312 – 0789
Vol. 22, No. 1, March (2026), pp. 30−43

Al-Khwarizmi Engineering Journal

Cefixime removal from wastewater by adsorption on activated carbon derived from broad bean peels using response surface methodology with Box–Behnken design

Huda Adil Sabbar
Department of Biochemical Engineering, Al-Khwarizmi College of Engineering, University of Baghdad, Baghdad-Iraq
Email: huda.adil@kecbu.uobaghdad.edu.iq

(Received 25 July 2024; Revised 8 October 2024; Accepted 2 December 2024; Published 1 March 2026)
https://doi.org/10.22153/kej.2026.12.012

Abstract

In this study, cefixime (CFX) was removed from aqueous solutions by using activated carbon (AC) made from broad bean peels (BBPs). To evaluate the adsorbent performance, a conventional experimental approach (one factor at a time) was applied to clarify the impact of the most influential variables (i.e., pH, contact time, and adsorbent dosage) and identify the maximum adsorption capacity. The optimization approach of response surface methodology with a Box–Behnken design (BBD) was employed to investigate the synergistic influences of the three independent variables and determine the optimum experimental conditions. Removal efficiency (%) was evaluated at different pH (2–10), contact time (10–150 min), and adsorbent dosage (0.1–2.5 g L^{-1}). Results revealed that the measurements adequately fitted the Langmuir isotherm, with a maximum monolayer adsorption capacity (qm) of 17.5 mg/g. Moreover, based on the optimization approach, 95% removal efficiency was reached at optimum values of 6, 100 min, and 2.16 for pH, contact time, and adsorbent dosage, respectively. The BET surface area was determined to be 375 m^2/g, and the total pore volume was 0.204 m^3/g. For multilayer sorption, the isotherm and kinetic models were suggested, followed by exothermic an physical adsorption mechanism. The findings of this study indicate that AC prepared from BBPs can be used as an adsorbent to remove CFX from aqueous solutions.

Keywords: *Optimization; Broad bean peels; Cefixime removal; Adsorption isotherm; Activated carbon*

1. Introduction

Water is a fundamental requirement for life, and the global demand for water grows at a rate of 1% annually [1–3]. Environmental pollution, especially water pollution, is a serious concern for researchers [4]. Antibiotics are extensively applied as medicine to improve human and animal health [5–8]; for example, cephalexin is often prescribed to treat bacterial infections. However, human and animal waste release significant amounts of antibiotics into the environment [9][10]. Traditional wastewater treatment technologies cannot completely remove released antibiotics [5]. Consequently, residual antibiotics in the wastewater have increased the resistance of pathogenic bacteria, posing a serious threat to surface water and groundwater [5,11,12].

Numerous studies have reported on the removal of antibiotic pollutants from wastewater, including chemical and biological processes [13–16]. Both approaches have their disadvantages: chemical processes such as membrane and advanced oxidation can be costly at large scale [17,18], while biological processes cannot be applied to remove antibiotics, as these pollutants can damage the microorganisms used in the treatment [19–21].

Adsorption can be considered more suitable than other technologies of antibiotic removal from wastewaters with pharmaceutical pollutants [22–26]. This technique offers several advantages in the effective removal of contaminants, such as a simple design and non-toxic residual generation [27–30]. Thus, in recent years, interest has increased in the preparation of activated carbon (AC) from inexpensive, renewable materials such as orange peels [31], tomato waste [17], and banana peels [32]. Broad beans are widely grown around the world, especially in the Mediterranean region [33]. Huge quantities of broad been peels (BBPs) are disposed, posing a serious environmental problem [34]. However, adsorption efficiency relies on several factors, the most crucial of which are adsorbent type, pH, adsorbent dose, and contact time [35,36].

In conventional approaches, tests are often performed by changing one parameter while others are fixed. As a result, the synergistic impact among all variables is missed. To address this gap, response surface methodology (RSM) has been utilized to determine the optimum experimental conditions and evaluate the interaction of experimental variables [37–39]. However, to the best of the author's knowledge, studies on using AC prepared from agricultural waste for cefixime (CFX) removal are rare in existing literature. Therefore, the main objective of this work was to investigate the possibility of using low-cost AC prepared from BBP wastes for removing CFX from aqueous solutions. To achieve this aim, the effects of solution pH, contact time, and adsorbent dosage on adsorption was evaluated systematically. Moreover, Langmuir, Freundlich, and Sips adsorption isotherms were applied, and the pseudo-first-order, pseudo-second-order, and pseudo-third-order models were used to explain the kinetics of CFX adsorption. RSM with BBD optimization was also utilized to determine the experimental design for investigating the synergistic effects of these three independent variables and determining the optimum experimental conditions.

2. Materials and Methods

2.1. Chemicals

All the chemicals used in this study were analytical grade, and distilled water was utilized to prepare all solution samples. The CFX (99%) used was purchased from Sigma-Aldrich. 0.5 N hydrochloric acid and 0.5 N sodium hydroxide were applied to adjust the pH of the solutions.

2.2. Preparation of Adsorbents from BBPs

The BBPs used in this work were produced locally in Iraq. They were first washed several times with distilled water to remove impurities such as dust. Then, the sample was dried in an oven for 24 h at 105 °C. The dried sample was crushed and thoroughly grounded using a mortar and pestle and then sieved to achieve particles 100–250 μm in size. To achieve carbonization, the sample was heated in an electrical furnace at 460 °C under a continuous flow of 150 mL min-1 of nitrogen for 2 hours. Afterward, the produced carbon was cooled to room temperature in the presence of nitrogen gas. Finally, the sample was rinsed using distilled water and 0.5 N HCl, and then dried for 12 h at 105 °C [40].

2.3. Characterization of BBP Charcoal

To distinguish the functional groups of AC derived from BBPs, Fourier transform infrared (FTIR) spectroscopy (Perkin Elmer Spectrum 100) was conducted in the wavenumber range of 4,000–400 cm^{-1}. Analyses of the AC were carried out by scanning electron microscopy (SEM) using a Zeiss Supra 40 (Germany).

2.4. Adsorption Experimental Method

Certain doses of AC adsorbents were added to 50 mL of the CFX solution and stirred for a specific time at 150 rpm. The solution pH was set at certain values by the addition of either 0.5 N HCl or 0.5 N NaOH. Next, the treated solution was centrifuged at 5,000 rpm and then filtered using Whatman™ filter paper to remove solid particles. The CFX concentration was analyzed using UV-vis spectrophotometry (Jasco V-670, JASCO Corporation, Japan) at 221 nm. All experiments were carried out in triplicate to achieve accurate measurements.

The adsorbent's CFX adsorption (qe) and removal efficiency (%) were calculated by applying the following equations [6] [41]:

$$q_e = \frac{(Co - Cf) \times V}{M\ (mg \times g - 1)} \quad \ldots(1)$$

$$\text{Removal efficiency } (\%) = \frac{(Co - Cf)}{Co} \times 100 \quad \ldots(2)$$

where V represents the volume of the CFX solution (L), M is the mass of the adsorbent (g), and C_0 and C_f are the initial and final concentrations of CFX in the solutions, respectively.

The data of the adsorption isotherms were fitted to the Langmuir and Freundlich models (Eqs. (3) and (4), respectively) [41–43] .

$$\frac{1}{q_e} = \frac{1}{K_L\, q_m} x \frac{1}{C_e} + \frac{1}{q_m} \quad \ldots(3)$$

$$\text{Ln } qe = \ln Kf + \left(\frac{1}{nf}\right) \ln Ce \quad \ldots(4)$$

$$\text{Ln}\left(\frac{qe}{qmax - qe}\right) = 1/n \ln Ce + \ln Ks \quad \ldots(5)$$

where Ce is the CFX concentration in the solution (mg L^{-1}), K_L is the Langmuir coefficient (L/mg), q_m is the maximum capacity (mg g^{-1}), and KF ((mg/g) $(L/mg)^{1/n}$) and n_f (dimensionless) are the respective nonlinear coefficients in Freundlich's equation, where KS is the constant of Sips (μg L^{-1}) -1/n and n (dimensionless).

Two common kinetic models were examined to mimic the adsorption kinetics of CFX and determine the adsorption kinetic mechanism. The pseudo-first-order and pseudo-second-order models (Eqs. (6) and (7), respectively) are among the kinetic equations commonly stated as follows [45]:

$$\ln (q_e - q_t) = \ln(k_1 qe) - k_1 t \quad \ldots(6)$$

$$\frac{1}{qt} = \left(\frac{1}{qe}\right) t + \left(\frac{1}{k2 \times qe\,2}\right) \quad \ldots(7)$$

The kinetic rate constants for the pseudo-first-order and pseudo-second-order models are denoted as k_1 (min^{-1}) and k^2 (g/mg.min), respectively. The variables q_t and q_e represent the adsorbed quantity (mg/g) at time t and at equilibrium, respectively. For the pseudo-first-order model, the values of k_1 and qe can be obtained from the slope and intercept of the ln (qe – qt) versus t plot, as given in Eq. (6). In the pseudo-second-order model, the constants k_2 and qe are determined by the slope and intercept of the 1/qt versus t plot, respectively.

RSM with BBD was employed to determine the best conditions for adsorption and identify the synergistic effects of three independent factors. pH (X_1), adsorbent dose (X_2) (g L^{-1}), and contact time (X_3) (min) were applied as the variables due to their significant influence on adsorption. To achieve the abovementioned objectives related to optimization, 15 tests were conducted by changing pH from 2 to 10, with a central point of 6; adsorbent dose from 0.1 g to 2.5 g, with a central point of 1.3 g; and contact time from 10 min to 100 min with a central point of 55 min. According to Eq. (8), the real values of independent factors (Xi) were represented as (xi) [46] follows:

$$x_1 = \frac{X_i - X_0}{\Delta X_i} \quad \ldots(8)$$

x_1 represents the actual value of variable X_i, X_0 represents the value of the actual variable at the center, and X_i represents the value of the step change.

The removal efficiency was predicted based on a second-order polynomial model (Eq. (9)) [47]:

$$Y = \beta_\circ + \sum_{j=1}^{K} \beta j \; Xj + \sum_{j=1}^{k} \beta jj \; X_j^2 + \sum_{j=1}^{k=1} \sum_{j=i+1}^{k} \beta ij \; XiXj + \varepsilon \quad \ldots(9)$$

where Y represents the expected removal efficiency, β_0 represents the constant, i and j represent the index number of patterns, k represents the number of variables, and βj, βjj, and βij represent the predicted coefficients based on regression analyses of linear, quadratic, and interaction impact, respectively. In the current study, Minitab (version 17) was employed to create the experiment with BBD.

3. Results and Discussion

3.1. Characterization of Adsorbents

SEM was applied to analyze the surface morphology of the prepared AC before and after adsorption (Figs. 1a and b, respectively). Fig. 1a illustrates that the surface of BBPs has a rough texture and an irregular microporous structure, which increases the performance of AC as an adsorbent. After CFX adsorption, a considerable change was detected in the surface structure of the BBPs (Fig. 1b), with binding sites covered by CFX molecules. Fig. 2 shows the FTIR spectrum of the AC. The peaks in the 1,000–1,300 cm^{-1} range can be due to the existence of C–C and C–O groups [21]. Moreover, the peak at 1500 cm^{-1} can be attributed to the ketone, aldehyde, and lactone groups [48], and the peak at 3,434.98 cm^{-1} can be linked to the O–H phenol functional groups [21] .

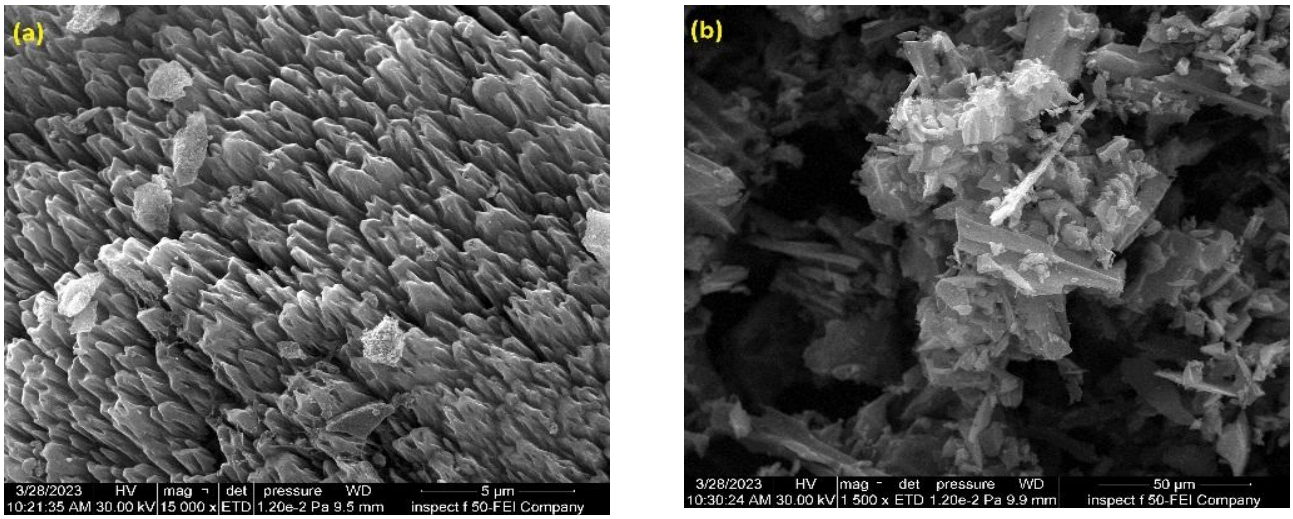

Fig. 1. SEM images of BBPs: (a) before adsorption and (b) after adsorption.

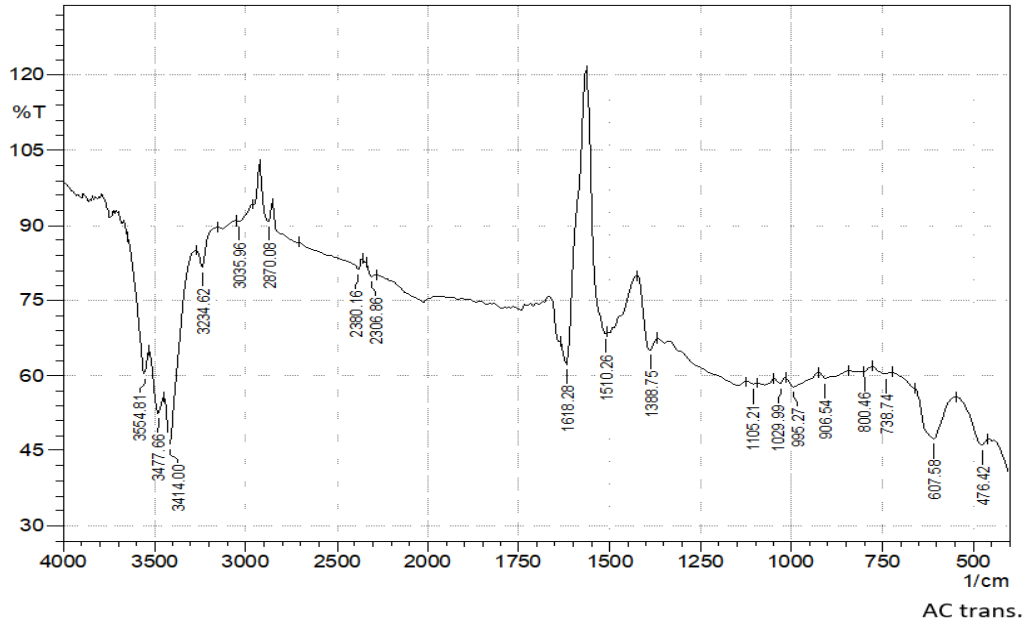

Fig. 2. FTIR spectra of BBPs after adsorption.

3.2. Evaluation of the Influence of Adsorption Parameters

3.2.1. Effect of Solution pH

Several batch tests were conducted to determine the appropriate variables for CFX adsorption by the AC adsorbent. The pH of the solution can be considered as the most significant variable in the adsorption system due to the specific functional groups of hydroniums [49]. Hence, the impact of pH was investigated using wide pH ranges (2–10), which were set by adding either 0.5 N HCl or 0.5 N NaOH in water as necessary. The removal efficiency of the absorbent is illustrated in Fig. 3. As shown in the figure, there is a strong relationship between removal efficiency and pH value. In regions with an acidic pH (2–4), CFX adsorption efficiency was found to be quite low. Clearly, the removal efficiency increased significantly between pH 4 and 7, and the highest CFX removal efficiency (83%) can be achieved at pH 7. Furthermore, CFX removal steadily declined in alkaline (pH > 7) conditions. These behaviors can be explained by the fact that at pH < 4 (acidic), functional groups with a positive charge on both the CFX solution and the adsorbent surface can be dominant, while functional groups with a negative charge on both the CFX solution and the surface of the adsorbent are dominant at pH > 7 (alkaline). Owing to the repulsive forces developed between like charges of the aqueous CFX solution and the adsorbent

surface, the adsorption capacity of CFX is thus decreased [21] [50].

3.2.2. Contact Time

The longest contact time between CFX adsorbate and adsorbent is crucial for investigating equilibrium adsorption due to the availability of functional groups present in the adsorbent [49] [51]. To measure effective contact time, 2.5 g of the AC adsorbent was mixed with a fixed initial concentration of CFX (50 mg L^{-1} at pH 7) for ranged time intervals. Fig. 4 depicts the relationship between removal efficiency and contact time. The results revealed that increased contact time enhanced the efficiency of adsorption. Furthermore, removal efficiency was high in the first time (70 min) intervals, slowed down, and then reached the highest value at equilibrium, which occurred after 80 min. This trend may be attributed to the functional group availability of the adsorbent [52]. This result is in line with past research [49] [53] [54].

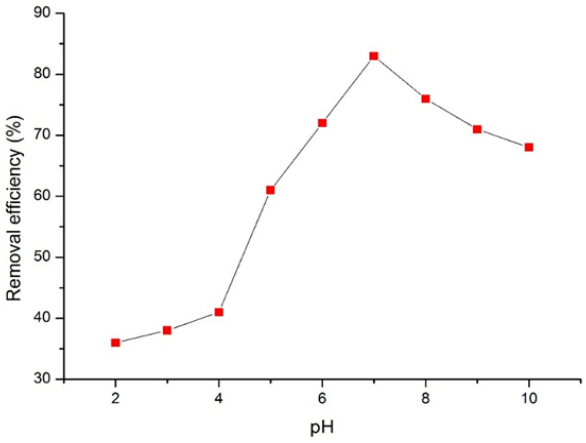

Fig. 3. Influence of solution pH on the removal efficiency of CFX (initial CFX concentration = 50 mg L–1, AC adsorbent dose = 2.5 g L-1, time = 70 min, and T = 25 °C).

3.2.3. Effect of AC Adsorbent Dose

The influence of the adsorbent dose of AC on removal efficiency was studied using different amounts of absorbent while the other experimental variables remained constant. Fig. 5 depicts the removal efficiency as a function of the adsorbent dose applied. The data demonstrated that the increased adsorbent dose significantly enhanced the adsorption efficiency up to a particular adsorbent dose (2 g L^{-1}), but beyond that the efficiency remained nearly constant. This behavior can be attributed to an increase in surface area and the availability of extra adsorption sites.

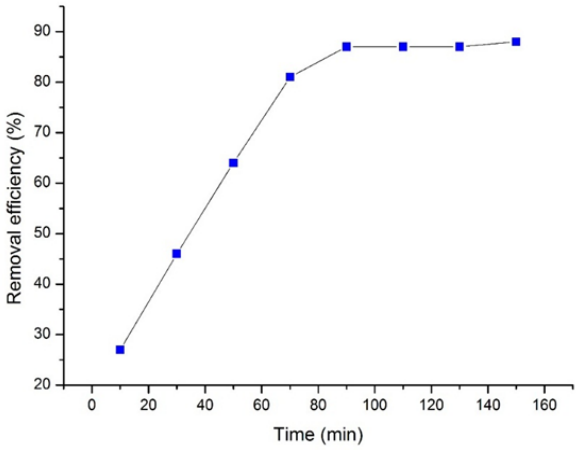

Fig. 4. Influence of contact time on the removal efficiency of CFX (initial CFX concentration = 50 mg L^{-1}, AC adsorbent dose = 2.5 g L^{-1}, pH = 7, and T = 25 °C).

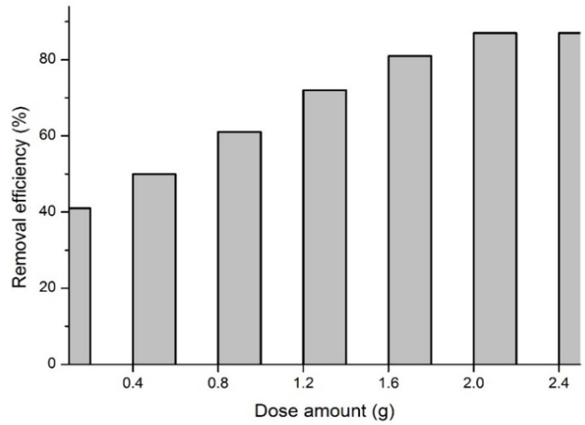

Fig. 5. Influence of AC adsorbent dose on the removal efficiency of CFX (initial CFX concentration = 50 mg L^{-1}, time = 90 min, pH = 7, and T = 25 °C).

3.3. Adsorption Isotherms

The relationship between the adsorbate in the solution and the adsorbate on the adsorbent can be described by the adsorption isotherm [55]. Langmuir, Freundlich, and Sips adsorption isotherms were employed to investigate the factors related to equilibrium. The Langmuir isotherm model can describe a homogenous adsorption in which adsorbates can be distributed in monolayer form. However, the Freundlich isotherm shows heterogeneous adsorption obtained from multilayers of adsorbates [56]. Based on Table 1, the maximum monolayer adsorption capacity (qm) is 17.5 mg/g. In addition, the value of the separation

factor (R_L) can be applied to determine whether adsorption can be favorable ($0 < R_L < 1$) or unfavorable ($R_L > 1$). In this study, R_L is 0.1282, demonstrating that CFX adsorption can be favorable. Fig. 6 reveals that the experimental data were adequately fitted to these models. The correlation coefficient (R_2) of the Langmuir, Freundlich, and Sips isotherm models are 0.9401 (Fig. 6a), 0.9273 (Fig. 6b), and 0.7331 (Fig. 6c), respectively. However, the constant n in the Freundlich model is higher than 1, indicating that CEX could be absorbed by AC. The findings of these study are compatible with those of earlier literature [4] [57].

Table 1,
Isotherm constants of Langmuir, Freundlich, and Sips for CFX adsorption using AC.

Langmuir			Freundlich			Sips			
q_m	K_L	R^2	K_F	N	R^2	qm	Ks	n	R^2
17.543	0.136	0.94019	2.106	1.439	0.92733	21.5	0.1908	0.5	0.73331

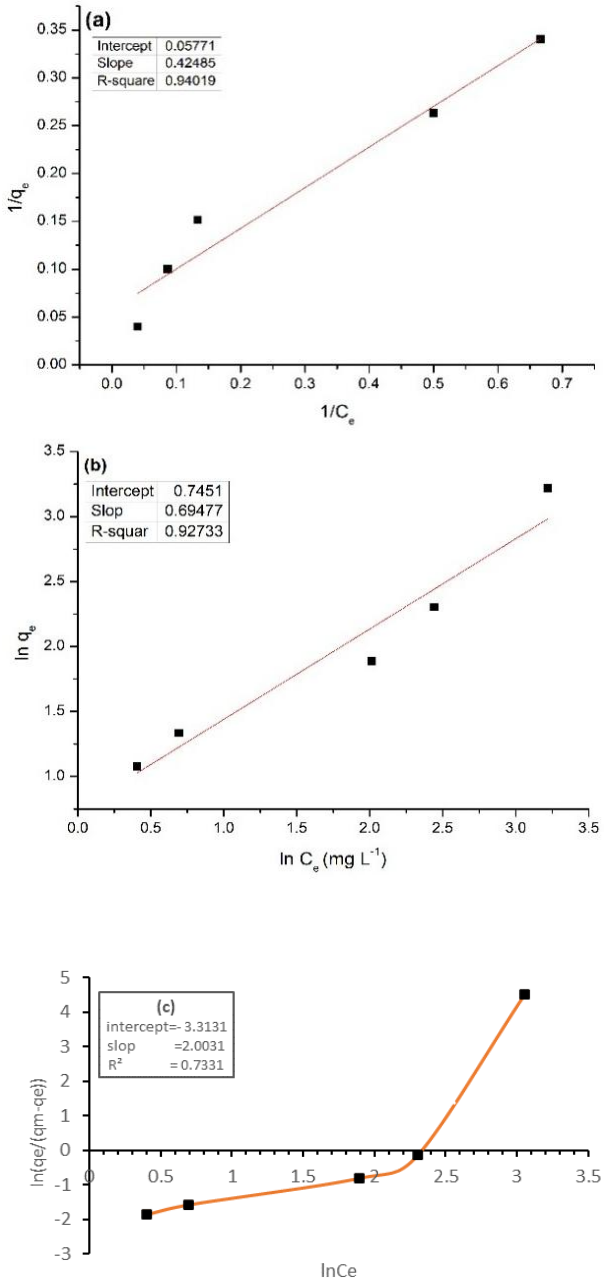

Fig. 6. Isotherm models: (a) Langmuir, (b) Freundlich, and (c) Sips.

3.4. Adsorption Kinetics

To characterize the adsorption mechanism and mass transfer rate on the surface or interior locations, kinetic models were used to evaluate the experimental data for contact time (Fig. 4). Three well-known models of pseudo-first- and pseudo-second-order were used to study the adsorption kinetics of CFX onto AC. As indicated in Figs. 7 and 8, the intercept and slope of the linearized version of the suggested models can be used to determine the values of the kinetic parameters [50].

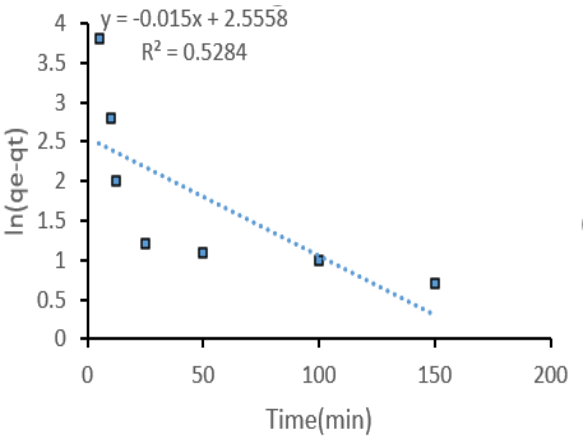

Fig. 7. Adsorption kinetic models for pseudo-first order.

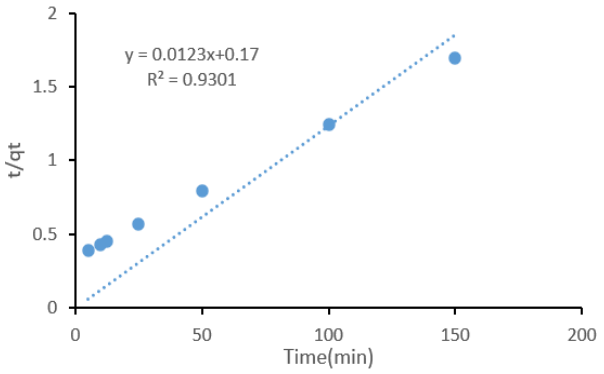

Fig. 8. Adsorption kinetic models for pseudo-second order.

Table 2 illustrates the kinetic models and their parameters, which are obtained from linear plots in Figs. 7 and 8. Regarding the R^2 values, the pseudo-second-order model (R^2 = 0.9999) fits the experimental data better than the pseudo-first-order (R^2 = 0.5418). The theoretical qe (calculated) based on the pseudo-second-order is also closer to the qe (experimental) compared with the pseudo-first order. Thus, a pseudo-second-order model applies to the evaluation of CFX kinetics onto the AC. Previous studies suggested that the pseudo-second-order model probably follows a chemical sorption mechanism for adsorption through electron sharing between analytes and adsorbents [58,59].

Table 2,
Pseudo-first-order, pseudo-second order, and intra-particle diffusion parameters for CFX adsorption (qe = 100.1 mg g^{-1}).

Model	Parameters	Cefixime
Pseudo first order	qe (mg/g)	12.91
K_1	(1/min)	0.015
R^2	-	0.5284
Pseudo first order	qe (mg/g)	81.3
K_2	(g/(mg·min))	0.000889
R^2	-	0.9301

3.5. Optimization of CFX Removal Using RSM with BBD

3.5.1 Multiple Regression Analyses

Synergistic effects among the three response parameters of CFX adsorption, including pH, adsorbent dose (g L^{-1}), and contact time (min), were evaluated. Specifically, multiple regression analysis was applied to generate second-order polynomial equations using the BBD matrix of actual measurements (Table 3):

Table 3,
Experimental and predicted values of removal efficiency using the BBD matrix.

	Actual values			Coded values				
Run No.	pH	Adsorbent dose (g)	Time (min)	x_1	x_2	x_3	Removal efficiency (%)	Predicted Removal efficiency (%)
1	2	0.1	55	-1	-2	0	79	78.7500
2	10	0.1	55	1	+1	0	84	83.0000
3	2	2.5	55	-1	+1	0	77	78.0000
4	10	2.5	55	+1	+1	0	80	80.2500
5	2	1.3	10	-1	0	-1	65	64.1250
6	10	1.3	10	+1	0	-1	75	74.8750
7	2	1.3	100	-1	0	+1	82	82.1250
8	10	1.3	100	+1	0	+1	77	77.8750
9	6	0.1	10	0	-1	-1	52	53.1250
10	6	2.5	10	0	+1	-1	72	71.8750
11	6	0.1	100	0	-1	+1	84	84.1250
12	6	2.5	100	0	+1	+1	63	61.8750
13	6	1.3	55	0	0	0	95	95.0000
14	6	1.3	55	0	0	0	95	95.0000
15	6	1.3	55	0	0	0	95	95.0000

$$\text{Removal efficiency (\%)} = 19.65 + 4.687\ x_1 + 30.20\ x_2 + 1.3711 x_3\ \ 0.2500\ x_1^2 - 7.639\ x_2^2 - 0.008025\ x_3^2 - 0.104\ x_1 .\ x_2 - 0.02083\ x_1 .\ x_3 - 0.1898\ x_1 .\ x_3 \quad \ldots(7)$$

here x_1, x_2, and x_3 represent coded values of pH, adsorbent dose (g L^{-1}), and contact time (min), respectively.

The obtained regression equation of the removal efficiency (%) with high determination coefficients (R^2) clarifies that this model can sufficiently describe the link among independent factors (pH, adsorbent dose, and contact time) and response (removal efficiency). The predicted values achieved by the suggested model were in reasonable agreement with the experimentally measured removal efficiency (Fig. 9).

3.5.2 Analysis of variance

Analysis of variance (ANOVA) of the second-order polynomial model and the significance for each model term are represented in Table 4. The p-value was utilized to check the significance. Statistically, the impact of the term is considered significant when its p-value is less than 0.05 [60]. As illustrated in Table 4, the coefficients of linear terms (x_1, x_2, and x_3) and of quadratic terms (x_1^2, x_2^2, and x_3^2) significantly influences the removal efficiency (%). In addition, the coefficients of interactive terms (x_1 . x_3 and x_2 . x_3) had a remarkable influence on the removal efficiency (%).

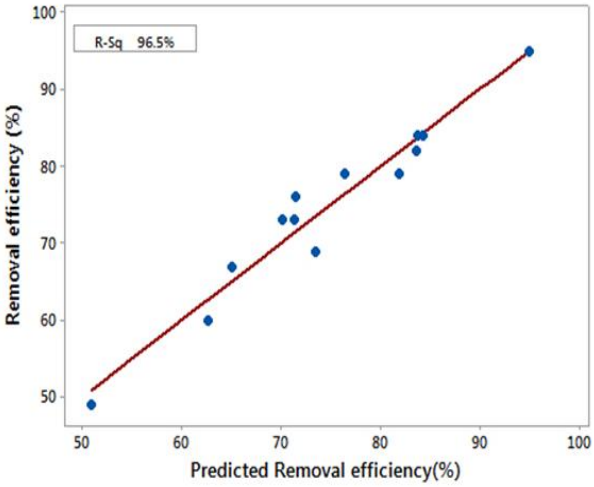

Fig. 9. Experimental values versus and predicted values of removal efficiency.

Table 4,
ANOVA analysis of BBD.

Model term	Sum of squares	Mean squares	F-Value	P-Value
X_1	21.12	21.125	16.9	0.09
X_2	6.13	6.125	4.90	0.038
X_3	220.50	220.500	176.40	0.002
X_1^2	59.08	59.077	47.26	0.001
X_2^2	446.77	446.769	357.42	0.000
X_3^2	975.00	975.000	780.00	0.003
$X_1 . X_2$	1.00	1.000	0.80	0.412
$X_1 . X_3$	56.25	56.250	45.00	0.001
$X_2 . X_3$	420.25	420.250	336.20	0.010

The 3-D response surface plots in Fig. 10 are based on Eq. (7), with one independent variable fixed at 0, while the other variables were adjusted within the selected variance for the experiments. These plots show the influence of pH, adsorbent dose, and contact time on removal efficiency. In Fig. 10, the removal efficiency was continuously increased along with the corresponding variables until the maximum adsorption was achieved, after which removal efficiency declined even when both variables were raised. For example, Fig. 10a shows that removal efficiency significantly improved when the pH increased from 2 to 7, and then gradually decreased when pH kept expanding from 7 to 10.

The optimal values of the independent variables for removal efficiency (%) were determined. The values of desired function range between 0 for completely undesired responses and 1 for completely acceptable response. The optimum values of pH, adsorbent dose, and contact time were identified to be 6, 2.16 g L^{-1}, and 100 min at 0.94

desirability, respectively. Under these optimum values, the predicted removal efficiency was 95%.

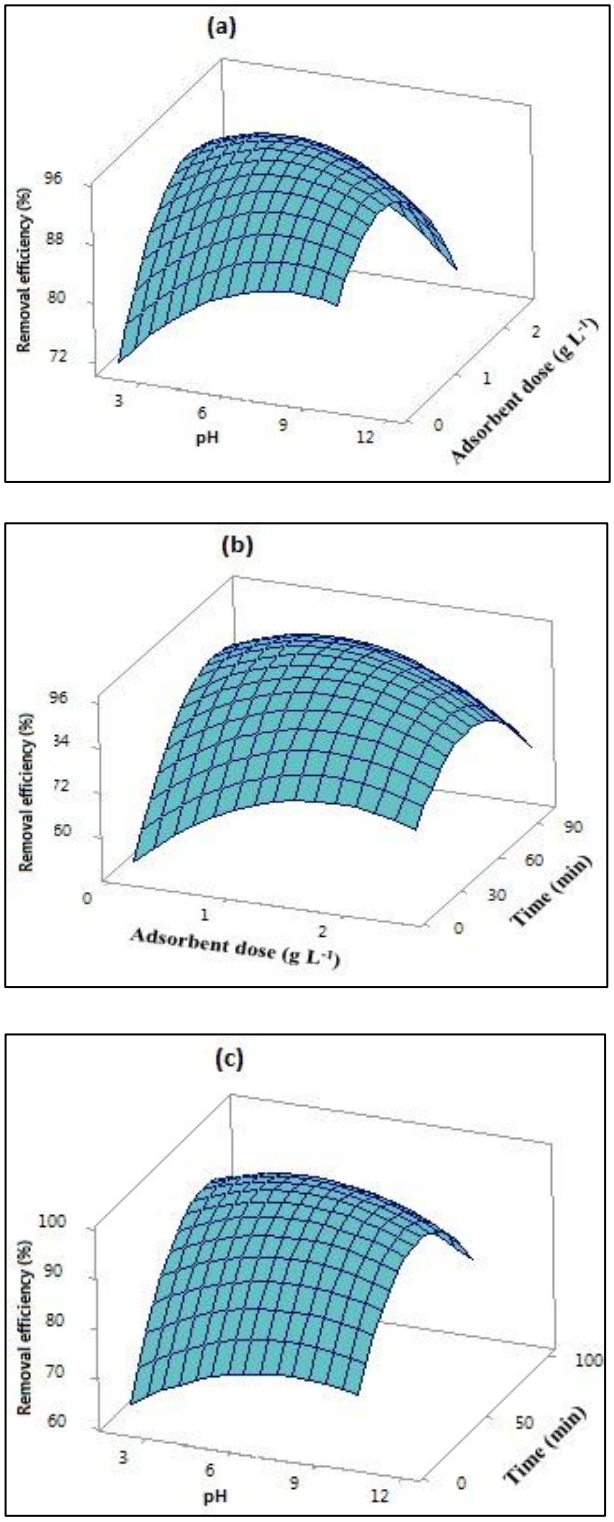

Fig. 10. Response surface plots of removal efficiency.

4. Conclusion

In this study, AC prepared from BBPs was applied to remove CFX from aqueous solutions. Results reveal that highest removal efficiency of 95% was achieved with the optimum values of pH 6, 2.16 g L^{-1} adsorbent dose, and 100 min contact time. In addition, the Langmuir isotherm model can offer higher fitting with the experimental data (0.94019), showing a homogenous and monolayer adsorption process. The findings of this study indicate that AC prepared from BBPs has considerable capacity for CFX removal. Thus, agricultural waste such as BBPs can be successfully used to prepare AC. The findings of this study can be utilized as baseline data for the design of treatments targeting effluents with cephalosporin substances, such as CFX.

Conflict of interest

The authors declare that there is no conflict of interest regarding the publication of this paper.

Abbreviations

CFX	Cefixime
AC	Activated carbon
BBPs	Broad bean peels
RSM	Response surface methodology
BBD	Box–Behnken design
FTIR	Fourier transform infrared spectroscopy
SEM	Scanning electron microscope
qe	Adsorbent capacity of CFX adsorption, mg g^{-1}
C0	Initial concentration of CFX in solution, mg L^{-1}
Cf	Final concentration of CFX in solution, mg L^{-1}
qm	Maximum adsorbent capacity of CFX adsorption, mg g^{-1}
KF	Nonlinear coefficient in Freundlich's equation
xi	Coded value for the actual value of variable
RL	Separation factor

References

[1] S. Rojas and P. Horcajada, "Metal-organic frameworks for the removal of emerging organic contaminants in water," Chem. Rev., vol. 120, no. 16, pp. 8378–8415, 2020, doi: 10.1021/acs.chemrev.9b00797

[2] C.-Y. Zhang and T. Oki, "Water pricing reform for sustainable water resources management in China's agricultural sector," Agric. Water Manag., vol. 275, p. 108045, 2023, doi: 10.1016/j.agwat.2022.108045.

[3] M. M. Jiad and A. H. Abbar, "Treatment of petroleum refinery wastewater by Sono Fenton process utilizing the in-situ generated hydrogen peroxide," Al-Khwarizmi Eng. J., vol. 19, no. 2, pp. 52–67, 2023, doi: 10.22153/kej.2023.04.002

[4] Y. C. Sharma and Uma, "Optimization of parameters for adsorption of methylene blue on a low-cost activated carbon," J. Chem. Eng. Data, vol. 55, no. 1, pp. 435–439, 2010, doi: 10.1021/je900408s.

[5] J. Yu, Y. Kang, W. Yin, J. Fan, and Z. Guo, "Removal of antibiotics from aqueous solutions by a carbon adsorbent derived from protein-waste-doped biomass," ACS Omega, vol. 5, no. 30, pp. 19187–19193, 2020, doi: 10.1021/acsomega.0c02568.

[6] M. M. M. Ali and M. J. Ahmed, "Adsorption behavior of doxycycline antibiotic on NaY zeolite from wheat (Triticum aestivum) straws ash," Journal of the Taiwan Institute of Chemical Engineers, vol. 81, pp. 218-224, 2017, doi: 10.1016/j.jtice.2017.10.026

[7] Y. Lu, M. Jiang, C. Wang, Y. Wang, and W. Yang, "Impact of molecular size on two antibiotics adsorption by porous resins," J. Taiwan Inst. Chem. Eng., vol. 45, no. 3, pp. 955–961, 2014.

[8] S. L. Kareem and A. A. Mohammed, "Removal of tetracycline from wastewater using circulating fluidized bed," Iraqi J. Chem. Petrol. Eng., vol. 21, no. 3, pp. 29–37, 2020, http://ijcpe.uobaghdad.edu.iq.

[9] Halling-Sørensen, S. N. Nielsen, P. F. Lanzky, F. Ingerslev, H. C. H. Lützhøft, and S. E. Jørgensen, "Occurrence, fate and effects of pharmaceutical substances in the environment-A review," Chemosphere, vol. 36, no. 2, pp. 357–393, 1998, doi: 10.1016/S0045-6535(97)00354-8.

[10] S. De Baere and P. De Backer, "Quantitative determination of amoxicillin in animal feed using liquid chromatography with tandem mass spectrometric detection," Analytica Chimica Acta, vol. 586, no. 1-2, pp. 319-325, 2007, doi: 10.1016/j.aca.2006.10.036

[11] V. Hasanzadeh, O. Rahmanian, and M. Heidari, "Cefixime adsorption onto activated carbon prepared by dry thermochemical activation of date fruit residues," Microchem. J., vol. 152, p. 104261, 2020, https://doi.org/10.1016/j.microc.2019.104261.

[12] P. Hongsawat and P. Prarat, "Comparative adsorption performance of oxytetracycline and sulfamethoxazole antibiotic on powder activated carbon and graphene oxide," Chem. Pap., vol. 76, no. 4, pp. 2293–2305, 2022, https://doi.org/10.1007/s11696-021-02024-9.

[13] F. J. Benitez et al., "Comparison of different chemical oxidation treatments for the removal of selected pharmaceuticals in water matrices," Chemical Engineering Journal, vol. 168, no. 3, pp. 1149-1156, 2011, doi: 10.1016/j.cej.2011.02.001.

[14] Ö. Uslu and I. A. Balcıoğlu, "Comparison of the ozonation and Fenton process performances for the treatment of antibiotic containing manure," Sci. Total Environ., vol. 407, no. 11, pp. 3450–3458, 2009

[15] Chatzitakis et al., "Photocatalytic degradation and drug activity reduction of chloramphenicol," Water Research, vol. 42, no. 1-2, pp. 386-394, 2008, doi: 10.1016/j.watres.2007.07.030.

[16] M. Jafari, S. F. Aghamiri, and G. Khaghanic, "Batch adsorption of cephalosporins antibiotics from aqueous solution by means of multi-walled carbon nanotubes," World Appl. Sci. J., vol. 14, no. 11, pp. 1642–1650, 2011.

[17] H. R. Pouretedal and N. Sadegh, "Effective removal of amoxicillin, cephalexin, tetracycline and penicillin G from aqueous solutions using activated carbon nanoparticles prepared from vine wood," J. Water Process Eng., vol. 1, pp. 64–73, 2014, doi: 10.1016/j.jwpe.2014.03.006.

[18] M. Xia, A. Li, Z. Zhu, Q. Zhou, and W. Yang, "Factors influencing antibiotics adsorption onto engineered adsorbents," J. Environ. Sci., vol. 25, no. 7, pp. 1291–1299, 2013

[19] M. S. Legnoverde, S. Simonetti, and E. I. Basaldella, "Influence of pH on cephalexin adsorption onto SBA-15 mesoporous silica: theoretical and experimental study," Appl. Surf. Sci., vol. 300, pp. 37–42, 2014, https://doi.org/10.1016/j.apsusc.2014.01.198.

[20] T. A. Cigu et al., "Adsorption and release studies of new cephalosporin from chitosan-g-poly (glycidyl methacrylate) microparticles," European Polymer Journal, vol. 82, pp. 132-

152, 2016, doi: 10.1016/j.eurpolymj.2016.07.011.
[21] D. Naghipour, A. Amouei, K. T. Ghasemi, and K. Taghavi, "Removal of cefixime from aqueous solutions by the biosorbent prepared from pine cones: Kinetic and isotherm studies," Desalination Water Treat., vol. 201, pp. 219–227, 2020, https://doi.org/10.5004/dwt.2020.26133.
[22] E. K. Putra, R. Pranowo, J. Sunarso, N. Indraswati, and S. Ismadji, "Performance of activated carbon and bentonite for adsorption of amoxicillin from wastewater: mechanisms, isotherms and kinetics," Water Res., vol. 43, no. 9, pp. 2419–2430, 2009, doi: 10.1016/j.watres.2009.02.039.
[23] G. Nazari, H. Abolghasemi, and M. Esmaieli, "Batch adsorption of cephalexin antibiotic from aqueous solution by walnut shell-based activated carbon," J. Taiwan Inst. Chem. Eng., vol. 58, pp. 357–365, 2016, https://doi.org/10.1016/j.jtice.2015.06.006.
[24] S. Bej et al., "Recent advancements on antibiotic bioremediation in wastewaters with a focus on algae: An overview," Environmental Technology, 2023, doi: 10.1080/09593330.2023.2245166.
[25] S. M. Al-Jubouri et al., "Silver oxide-zeolite for removal of an emerging contaminant by simultaneous adsorption-photocatalytic degradation under simulated sunlight irradiation," Journal of Photochemistry and Photobiology A: Chemistry, vol. 442, p. 114763, 2023, doi: 10.1016/j.jphotochem.2023.114763.
[26] M. Azizpourian, G. Kouchakzadeh, and Z. Derikvand, "Removal of pharmaceutical compounds from aqueous solution by clay-based synthesized adsorbents: adsorption kinetics and isotherms studies," Chemical Papers, vol. 77, no. 8, pp. 4245-4264, 2023, doi: 10.1007/s11696-023-02774-8.
[27] R. Khazaei, A. Rahmani, A. Seidmohammadi, J. Faradmal, and M. Leili, "Evaluation of the efficiency of photocatalytic UV/peroxymonosulfate process in the removal of cefixime antibiotic from aqueous solutions," Sci. J. Kurdistan Univ. Med. Sci., vol. 24, no. 4, pp. 22–40, 2019.
[28] Z. Aksu and Ö. Tunç, "Application of biosorption for penicillin G removal: comparison with activated carbon," Process Biochemistry, vol. 40, no. 2, pp. 831-847, 2005, doi: 10.1016/j.procbio.2004.03.009.
[29] K. E. Talib and S. D. Salman, "Removal of malachite green from aqueous solution using Ficus Benjamina activated carbon-nonmetal oxide synthesized by pyro carbonic acid microwave," Al-Khwarizmi Eng. J., vol. 19, no. 2, pp. 26–38, 2023, doi: 10.22153/kej.2023.03.002.
[30] M. W. Khalid and S. D. Salman, "Adsorption of heavy metals from aqueous solution onto sawdust activated carbon," Al-Khwarizmi Eng. J., vol. 15, no. 3, pp. 60–69, 2019, doi: 10.22153/kej.2019.04.001.
[31] M. E. Fernandez et al., "Development and characterization of activated hydrochars from orange peels as potential adsorbents for emerging organic contaminants," Bioresource Technology, vol. 183, pp. 221-228, 2015, doi: 10.1016/j.biortech.2015.02.035.
[32] P. Nowicki, J. Kazmierczak-Razna, and R. Pietrzak, "Physicochemical and adsorption properties of carbonaceous sorbents prepared by activation of tropical fruit skins with potassium carbonate," Mater. Des., vol. 90, pp. 579–585, 2016, doi: 10.1016/j.matdes.2015.11.004.
[33] E. D. Miguel Gordillo, El garbanzo: una alternativa para el secano, Mundi-Prensa, 1991.
[34] H. Hameed and M. I. El-Khaiary, "Sorption kinetics and isotherm studies of a cationic dye using agricultural waste: Broad bean peels," J. Hazard. Mater., vol. 154, no. 1–3, pp. 639–648, 2008, doi: 10.1016/j.jhazmat.2007.10.081.
[35] D. Naghipour, A. Amouei, M. Estaji, K. Taghavi, and A. Allahabadi, "Cephalexin adsorption from aqueous solutions by biochar prepared from plantain wood: equilibrium and kinetics studies," Desalination Water Treat., vol. 143, pp. 374–381, 2019, https://doi.org/10.5004/dwt.2019.23563.
[36] J. Rivera-Utrilla, G. Prados-Joya, M. A. Sánchez-Polo, M. A. Ferro-García, and I. Bautista-Toledo, "Removal of nitroimidazole antibiotics from aqueous solution by adsorption/bioadsorption on activated carbon," J. Hazard. Mater., vol. 170, no. 1, pp. 298–305, 2009, doi: 10.1016/j.jhazmat.2009.04.096.
[37] H. H. Al-Mohammedawi, H. Znad, and E. Eroglu, "Synergistic effects and optimization of photo-fermentative hydrogen production of Rhodobacter sphaeroides DSM 158," International Journal of Hydrogen Energy, vol. 43, no. 33, pp. 15823-15834, 2018, doi: 10.1016/j.ijhydene.2018.06.140.
[38] N. M. Alawi et al., "Optimization of discharge plasma reactor for dry reforming of methane using response surface methodology," Bulletin of Chemical Reaction Engineering &

Catalysis, vol. 11, 2023, doi: 10.9767/bcrec.11.2.12345.67890

[39] Vohra, M. Hussaini, and T. Mohammad, "Olive branches activated carbon: Synthesis, phenol adsorption and modeling," Chem. Pap., vol. 77, no. 1, pp. 485–498, 2023, doi: 10.1007/s11696-022-02457-w.

[40] Y. X. Gan, "Activated carbon from biomass sustainable sources," C, vol. 7, no. 2, p. 39, 2021, https://doi.org/10.3390/c7020039

[41] K. Hummadi, "Optimal operating conditions for adsorption of heavy metals from an aqueous solution by an agriculture waste," Iraqi J. Chem. Petrol. Eng., vol. 22, no. 2, pp. 27–35, 2021, https://doi.org/10.31699/IJCPE.2021.2.4

[42] R. G. Yousuf, H. A. Sabbar, and Z. Y. Atiyah, "Utilizing waste mango and avocado seeds for highly effective dye removal with activated carbon," Asia-Pacific J. Mol. Biol. Biotechnol., vol. 31, no. 2, pp. 71–79, 2023.

[43] M. H. M. Ali, R. F. Almilly, and R. K. Abid, "Isotherms and kinetics study for adsorption of nitrogen from air using zeolite Li-LSX to produce medical oxygen," Iraqi Journal of Chemical and Petroleum Engineering, vol. 24, no. 2, pp. 81-87, 2023, doi: 10.31699/IJCPE.2023.2.9

[44] B. Lim, N. Priyantha, H. H. Cheng, N. A. H. M. Zaidi, and G. Link, "Parkia speciosa (Petai) pod as a potential low-cost adsorbent for the removal of toxic crystal violet dye," Scientia Bruneiana, vol. 15, pp. 99–106, 2016.

[45] L. X. Dinh et al., "The adsorption kinetic and isotherm studies of metal ions (Co2+, Sr2+, Cs+) on Fe3O4 nanoparticle of radioactive importance," Results in Chemistry, vol. 101095, 2023, doi: 10.1016/j.rechem.2023.101095.

[46] W. Boumyaa et al., "Box–Behnken design for understanding of adsorption behaviors of cationic and anionic dyes by activated carbon," Molecules, vol. 15, pp. 17-19, 2021, doi: 10.5004/dwt.2021.26610.

[47] S. Alkorbi, M. Tanveer, H. Shahid, M. B. Qadir, F. Ahmad, Z. Khaliq, and F. A. Harraz, "Comparative analysis of feed-forward neural network and second-order polynomial regression in textile wastewater treatment efficiency," AIMS Mathematics, vol. 9, no. 5, pp. 10955-10976, 2024.

[48] M. N. Hasan, M. A. Shenashen, M. M. Hasan, H. Znad, and M. R. Awual, "Assessing of cesium removal from wastewater using functionalized wood cellulosic adsorbent," Chemosphere, vol. 270, p. 128668, 2021, https://doi.org/10.1016/j.chemosphere.2020.128668

[49] M. N. Hasan, M. A. Shenashen, M. M. Hasan, H. Znad, and M. R. Awual, "Assessing of cesium removal from wastewater using functionalized wood cellulosic adsorbent," Chemosphere, vol. 270, p. 128668, 2021, doi: 10.1016/j.chemosphere.2020.128668.

[50] M. E. Esmaeili Bidhendi et al., "Nano-size biomass derived from pomegranate peel for enhanced removal of cefixime antibiotic from aqueous media: kinetic, equilibrium and thermodynamic study," International Journal of Environmental Research and Public Health, vol. 17, no. 12, p. 4223, 2020, doi: 10.3390/ijerph17124223.

[51] Islam et al., "Advances in sustainable approaches to recover metals from e-waste-A review," J. Clean. Prod., vol. 244, p. 118815, 2020, doi: 10.1016/j.jclepro.2019.118815.

[52] M. N. Arshad et al., "Fabrication of cadmium ionic sensor based on (E)-4-Methyl-N′-(1-(pyridin-2-yl) ethylidene) benzenesulfonohydrazide (MPEBSH) by electrochemical approach," Journal of Organometallic Chemistry, vol. 827, pp. 49-55, 2017, doi: 10.1016/j.jorganchem.2016.11.009.

[53] M. Mazrouaa et al., "Nano-composite multi-wall carbon nanotubes using poly (p-phenylene terephthalamide) for enhanced electric conductivity," J. Environ. Chem. Eng., vol. 7, no. 2, p. 103002, 2019, https://doi.org/10.1016/j.jece.2019.103002.

[54] F. Mohammadi, N. Moradpour, N. Azimi, and E. Ebrahimi, "Feasibility of the purification of pharmaceuticals from aqueous solutions using carbon nanotubes in the presence of oxidizers," Iranian J. Chem. Eng., vol. 21, no. 2, pp. 43–55, 2024, https://doi.org/10.22034/ijche.2024.443106.1523.

[55] T. A. Saleh, "Isotherm models of adsorption processes on adsorbents and nanoadsorbents," in Interface Sci. Technol., vol. 34, pp. 99–126, Elsevier, 2022, doi: 10.1016/B978-0-12-849876-7.00009-9

[56] Gupta and R. K. Vyas, "Evaluation of acyclovir adsorption on granular activated carbon from aqueous solutions: batch and fixed-bed parametric studies," Chemical Papers, vol. 77, no. 8, pp. 4599-4612, 2023, doi: 10.1007/s11696-023-02810-7.

[57] G. Annadurai, R.-S. Juang, and D.-J. Lee, "Use of cellulose-based wastes for adsorption of dyes from aqueous solutions," Journal of

Hazardous Materials, vol. 92, no. 3, pp. 263-274, 2002, doi: 10.1016/S0304-3894(02)00017-1

[58] Ghodbane and O. Hamdaoui, "Removal of mercury (II) from aqueous media using eucalyptus bark: Kinetic and equilibrium studies," Journal of Hazardous Materials, vol. 160, pp. 301-309, 2008, doi: 10.1016/j.jhazmat.2008.02.116.

[59] G. M. S. Uddin, S. Saha, S. Karmaker, and T. K. Saha, "Adsorption of cefixime trihydrate onto chitosan 10b from aqueous solution: Kinetic, equilibrium and thermodynamic studies," Adsorption, vol. 6, p. 9, 2021.

[60] H. F. Hameed, A. K. Mohammed, and D. S. Zageer, "Comparative study between activated carbon and charcoal for the development of latent fingerprints on nonporous surfaces," Al-Khwarizmi Eng. J., vol. 18, no. 4, pp. 1–13, 2022, doi: 10.22153/kej.2022.09.001.

إزالة السيفيكسيم من مياه الصرف الصحي عن طريق الامتزاز على الكربون المنشط المشتق من قشور الفول باستخدام منهجية سطح الاستجابة مع تصميم Box-Behnken

هدى عادل صبار
قسم الهندسة الكيميائية الاحيائية / كلية هندسة الخوارزمي / جامعة بغداد/ بغداد/ العراق
البريد الالكتروني:huda.adil@kecbu.uobaghdad.edu.iq

المستخلص

في هذه الدراسة، تمت إزالة السيفيكسيم (CFX) من المحاليل المائية باستخدام الكاربون المنشط (AC) المحضر من قشور الباقلاء BBPS. وتم تطبيق المنهج التجريبي (عامل واحد في كل مرة لتوضيح العامل الأكثر تأثيراً والتعرف على أكبر قدرة للامتصاص بمن ثم تقييم أداء المواد المازة. في هذا المنهج التقليدي تم فحص الرقم الهيدروجيني (٢-١)، ووقت التلامس (١٠-١٥٠ دقيقة) وكمية المادة المازة (٠,١-٢,٥) غم لكل لتر. بعد ذلك، تم استخدام أعلى منهجية سطح الاستجابة (RMS) مع التصميم التجريبي Box-Behnken (BBD) ودراسة التأثير المتداخل لثلاثة متغيرات بصورة مستقلة، وتحديد الظروف التجريبية المثلى في تحقيق أعلى إزالة والنسبة المئوية المتحققة في الظروف المختلفة من الرقم الهيدروجيني (٢-١٠)، ووقت الاتصال (١٠-١٠٠ دقيقة)، وجرعة المادة الماصة (٠,١-٢,٥ جم لتر-١). إذ إن النتائج بينت أن القياسات تتلاءم بشكل مناسب مع لا تغموير المتساوية في درجة الحرارة وقد وجد أعلى قدرة امتصاص للطبقة الأحادية يشير إلى ١٧,٥ ملغم / غم. إضافة الى ذلك، الاعتماد على منهج الامثلية، كانت الفعالة في الإزالة ٩٥٪ عند القيم المثلى التي هي وقت التلامس ٦ و ١٠٠ دقيقة و ٢,١٦ لدرجة الحموضة وجرع المادة المازة على التوالي توضح نتائج هذه الدراسة أنّه يمكن استخدام الكاربون المنشط المحضر من BBPS كمادة ماصة فعال لإزالة CFX من المحاليل المائية.